Iranian Journal of Materials Science and Engineering, Vol. 21, Number 3, September 2024
RESEARCH PAPER

Investigation of the Simultaneous Effect of Electrolyte Additives and α-PbO_2 Intermediate Layer on the Electrodeposition of Ti/β-PbO_2 Electrode

Hadi Sharifidarabad, Alireza Zakeri, Mandana Adeli*

* *adelim@iust.ac.ir*

[1] Metal Extraction Research Laboratory, School of Metallurgy and Materials Engineering, Iran University of Science and Technology, Narmak 1684613114, Tehran, Iran

Received: January 2024 **Revised: April 2024** **Accepted: August 2024**
DOI: 10.22068/ijmse.3513

Abstract: *The sensitivity of lead dioxide coating properties to the deposition conditions and electrolyte composition has allowed the preparation of coatings with different properties for different applications. In this study, the effects of electrolyte additives on the electrodeposition process were investigated using electrochemical measurements such as cyclic voltammetry, chronoamperometry, and electrochemical impedance spectroscopy. The results showed that the presence of fluoride ions significantly reduces the possibility of TiO_2 formation. The addition of copper ions not only prevents lead loss at the cathode but also leads to the formation of copper oxide on the surface at the initial stages, which hinders nucleation of PbO_2. The presence of sodium dodecyl sulfate (SDS) also interferes with the nucleation process as it occupies active nucleation sites. The α-PbO_2 interlayer prevents copper oxidation and solves the problem of lead dioxide nucleation. Finally, it was found that the simultaneous use of all additives together with the α-PbO_2 interlayer has a positive effect on the coating process.*

Keywords: *Lead dioxide electrode, Anodic electrodeposition, Chronoamperometry, Cyclic voltammetry.*

1. INTRODUCTION

The lead dioxide electrode has been known as one of the most widely used electrodes since the invention of the lead-acid battery [1]. PbO_2 electrodes exhibit unique properties that distinguish them from other anodes, such as low cost [2, 3], high chemical stability [4, 5], and electrocatalytic activity [6, 7]. PbO_2 electrodes, which are primarily fabricated by anodic deposition [8, 9], have received more attention from researchers and industry professionals. Lead dioxide has two crystal structures (α-PbO_2 and β-PbO_2), each with unique properties [10, 11]. The electrocatalytic properties and chemical stability of lead dioxide electrodes can be modified and customized according to the desired application by controlling the synthesis conditions and using different additives [12-14]. Therefore, PbO_2 electrodes are not only used in the field of energy storage [15], but also in the production of ozone [16, 17], wastewater treatment [18-20], and recently in the electrowinning of non-ferrous metals [21-24].

Numerous studies have been conducted to better understand the details of the electrochemical mechanism of lead dioxide electrodeposition [25-27]. Currently, the model proposed by Velichenko et al. for lead dioxide coating in an acidic environment is widely accepted among researchers [27-29]. According to their proposed mechanism, the role of hydroxyl radicals (OH) formed during the coating process by decomposition of water is considered crucial for the anodic deposition of lead dioxide. Reactions (1-4) represent this model.

$$H_2O \rightarrow OH_{ads} + H^+ + e^- \quad (1)$$
$$Pb^{2+} + OH_{ads} \rightarrow Pb(OH)^{2+} \quad (2)$$
$$Pb(OH)^{2+} + H_2O \rightarrow Pb(OH)_2{}^{2+} + H^+ + e^- \quad (3)$$
$$Pb(OH)_2{}^{2+} \rightarrow PbO_2 + 2H^+ \quad (4)$$

Based on these reactions, the mechanism of lead dioxide formation on the substrate proceeds in four steps. When a current is applied, a quantity of OH radicals is formed and adsorbed on the surface of the anode. This substance reacts with Pb^{2+} ions present in the electrolyte to form $Pb(OH)^{2+}$, which is then electrochemically converted to $Pb(OH)_2{}^{2+}$. In the final step, the lead dioxide chemically crystallizes at the electrode surface [29]. Thus, the coating of the lead dioxide on the anode surface is a two-electron transfer process that has no relation to the electrolyte medium. This means that the additives to the electrolyte only affect the kinetics of the process [6, 16].

In a study by Shen et al. [30], the electrodeposition process of lead dioxide on the titanium surface was investigated using a cyclic

[DOI: 10.22068/ijmse.3513]

voltammetry method. They showed that deposition starts at a voltage of 1.9 V, indicating the formation of the lead dioxide layer and the oxygen evolution reaction. In the second cycle, the initiation of the anodic peak occurred at 1.7 V, meaning that the subsequent formation of lead dioxide on the deposited PbO_2 surface is easier. In another study by Chen et al. [10], the process of lead dioxide electrode formation on aluminum substrate was investigated in both acidic and alkaline environments. According to their study deposition of alpha phase (alkaline environment) starts above 0.25 V with two anodic peaks at 0.29 V and 0.49 V, respectively on aluminum substrate, indicating the formation of Pb_3O_4 and PbO_2 phases. Moreover, the cathodic peak at 0.1 V represents the dissolution of the previously formed cathodic phase of lead dioxide. Also, the potential for initiating the deposition of the beta phase (acidic environment) was about 1.66 V, which means that lead dioxide forms much faster in an alkaline environment than in an acidic environment. In addition to the study of lead dioxide electrodeposition, numerous efforts have been made to improve the performance of lead dioxide coatings through various additives. Reports have shown that using additives can significantly improve the stability and electrocatalytic properties of lead dioxide coatings. Various additives have been applied to the electrodeposition bath in the form of ions and oxide particles such as F^- [31], Bi^{3+} [32], Ag^+ [33], Cu^{2+} [34], MnO_2 [35], ZrO_2 [12], RuO_2 [36], Co_3O_4 [37] to improve the performance of lead dioxide electrodes. Table 1 shows a list of selected additives and their advantages in lead dioxide electrodeposition. All these studies show that additives may have significant effects on the morphology, structure, electrochemical properties, and stability of lead dioxide deposits. Despite all these studies, the simultaneous usage of additives in the electrodeposition process of lead dioxide electrodes has not been attempted so far. In addition, the effects of surfactants, such as sodium dodecyl sulfate (SDS), and their composite formation with oxides on the electrodeposition of lead dioxide have been studied, but their individual effects have not been evaluated. In our previous study [43], the effects of Cu^{2+}, SDS, and the presence of α-PbO_2 interlayer on the properties of Ti/α-PbO_2/β-PbO_2 anode suitable for electrowinning applications were evaluated. It was found that the presence of all additives improved the electrocatalytic activity and stability of the electrode and decreased the oxygen evolution potential (OEP) of the electrode from 2.05 to 1.85 V which is beneficial for electrowinning applications. In this study, the separate and combined effects of fluoride ions, copper ions, SDS, and an α-PbO_2 intermediate layer on the electrodeposition process of lead dioxide were investigated using cyclic voltammetry (CV), chronoamperometry (CA) and electrochemical impedance spectroscopy (EIS) to gain a better understanding of the effects of these additives on the properties of the prepared lead dioxide anode to be used in electrowinning processes.

2. EXPERIMENTAL PROCEDURES

2.1. Electrode Preparation

The titanium plates were cut to dimensions of 25 × 25 × 0.6 mm and polished with sandpaper (400-800 mesh number). The polished Ti plates were then degreased by washing the surface with soap and immersing them in a soap-water mixture for 30 min, followed by washing with deionized water and another 30 minutes of immersion in ultra-pure acetone. Then the Ti plate was etched in boiling 15 wt% oxalic acid for 1 hour until the surface of the Ti plate turned gray. Finally, they were washed thoroughly with distilled water and stored in ultra-pure isopropanol.

Table 1. A list of selected additives and their advantages for lead dioxide electrodes

Additive	Effect	Ref.
F^-	increases stability	[38]
Cu^{2+}	prevents lead waste on the cathode, reduces grain size, increases coating density	[34]
Ce^{3+}	increases stability, improves electrocatalytic activity	[39]
Fe^{3+}	increases deposition rate, improves electrocatalytic activity	[40]
Co^{2+}	improves electrocatalytic activity	[41]
ZrO_2	Increases stability, increases oxygen evolution potential (OEP)	[41]
Co_3O_4	improves electrocatalytic activity and active surface area	[42]

[DOI: 10.22068/ijmse.3513]

Prepared Ti samples were used as the working electrode (anode), while Pt sheets were used as the counter electrode (cathode).

2.2. Electrochemical Measurements

The electrochemical measurements were performed on the CorrTest Electrochemical Workstation CS350. Ti samples with dimensions of 25 × 25 mm and a working area of 2 cm^2 were used as the working electrode, while Ag/AgCl and Pt sheet were used as the reference and the counter electrode, respectively. Cyclic voltammetry was performed with a potential range of 0 to 2.5 V for 2 cycles with a scan rate of 20 mV/s. Chronoamperometry experiments were carried out with single positive potential steps from the open-circuit potential to 1.8 V vs. Ag/AgCl. Electrochemical impedance spectroscopy (EIS) was measured at 1.8 V vs. Ag/AgCl at frequencies ranging from 100 kHz to 100 MHz.

For all electrochemical measurements, the composition of the electrodeposition bath included 0.5 $mol.L^{-1}$ $Pb(NO_3)_2$, 0.1 $mol.L^{-1}$ HNO_3, and different kinds of additives as needed (0.05 $mol.L^{-1}$ NaF, 0.026 $mol.L^{-1}$ $Cu(NO_3)_2$ and 0.001 $mol.L^{-1}$ SDS) (Table 2). All chemicals used were of high purity and analytical grade. Scanning electron microscopy (VEGA TESCAN, Czech Republic) was performed to study the microstructure and morphology of the samples.

3. RESULTS AND DISCUSSION

3.1. Effects of Additives on Cyclic Voltammetry Curves

To study the process of lead dioxide coating on the titanium substrate in different deposition environments, the coating was carried out using cyclic voltammetry. The prepared titanium substrate was considered as the working electrode, while a Pt sheet and an Ag/AgCl electrode were used as the counter and reference electrodes, respectively. Cyclic voltammetry in the range of 0-2.5 V with a scan rate of 20 mV/s in different environments was used to study the process of lead dioxide deposition (Fig. 1).

Fig. 1(a) shows the cyclic voltammetry curve of Ti substrate in 0.1 M nitric acid solution in the presence of 0.5 M $Pb(NO_3)_2$ without any additives (Sample A2). It should be noted that the substrate was cycled without preparation or interruption between cycles. With an increase in potential, no significant changes in current were observed until the onset potential (E_{onset}) of PbO_2 formation (p1) at 1.9 V, where the current density increased exponentially afterward. This exponential increase indicates the deposition of PbO_2 on the titanium substrate and the evolution of oxygen [10, 12]. In the potential reversal path, the oxidation reaction continues up to a voltage of 1.75 V (p2). This is due to the ease of continued coating on the already-formed PbO_2 layer compared to the titanium substrate [44]. A cathodic peak (c1) is observed at 0.44 V, which is due to the reduction of the freshly formed PbO_2 [10, 12]. It is important to note that the current density on the reverse path is still negative, indicating the presence of a PbO_2 layer on the titanium surface [45]. The second cycle is similar to that of the first cycle, with the difference that the E_{onset} is 1.8 V, which is 0.1 V lower than the first cycle. Also in the second cycle, an anodic peak (a1) is observed before the E_{onset} in the potential range of 1.2-1.6 V, which is attributed to the oxidation of PbO to PbO_2 [43]. A cathodic peak (c2) is observed at 0.46 V, with the difference that the current density is significantly reduced compared to c1, which could be due to the increased stability and adhesion of the PbO_2 coated on the already formed lead dioxide.

Table 2. Details of the samples and additives used in each sample

Sample Code	Substrate	Additive	Concentration of additive ($mol.L^{-1}$)
A2	Ti	-	-
B2	Ti	NaF	0.05
C2	Ti	NaF $Cu(NO_3)_2$	0.05 0.026
D2	Ti	NaF $Cu(NO_3)_2$ SDS	0.05 0.026 0.001
E2	Ti/α-PbO_2	NaF $Cu(NO_3)_2$ SDS	0.05 0.026 0.001

[DOI: 10.22068/ijmse.3513]

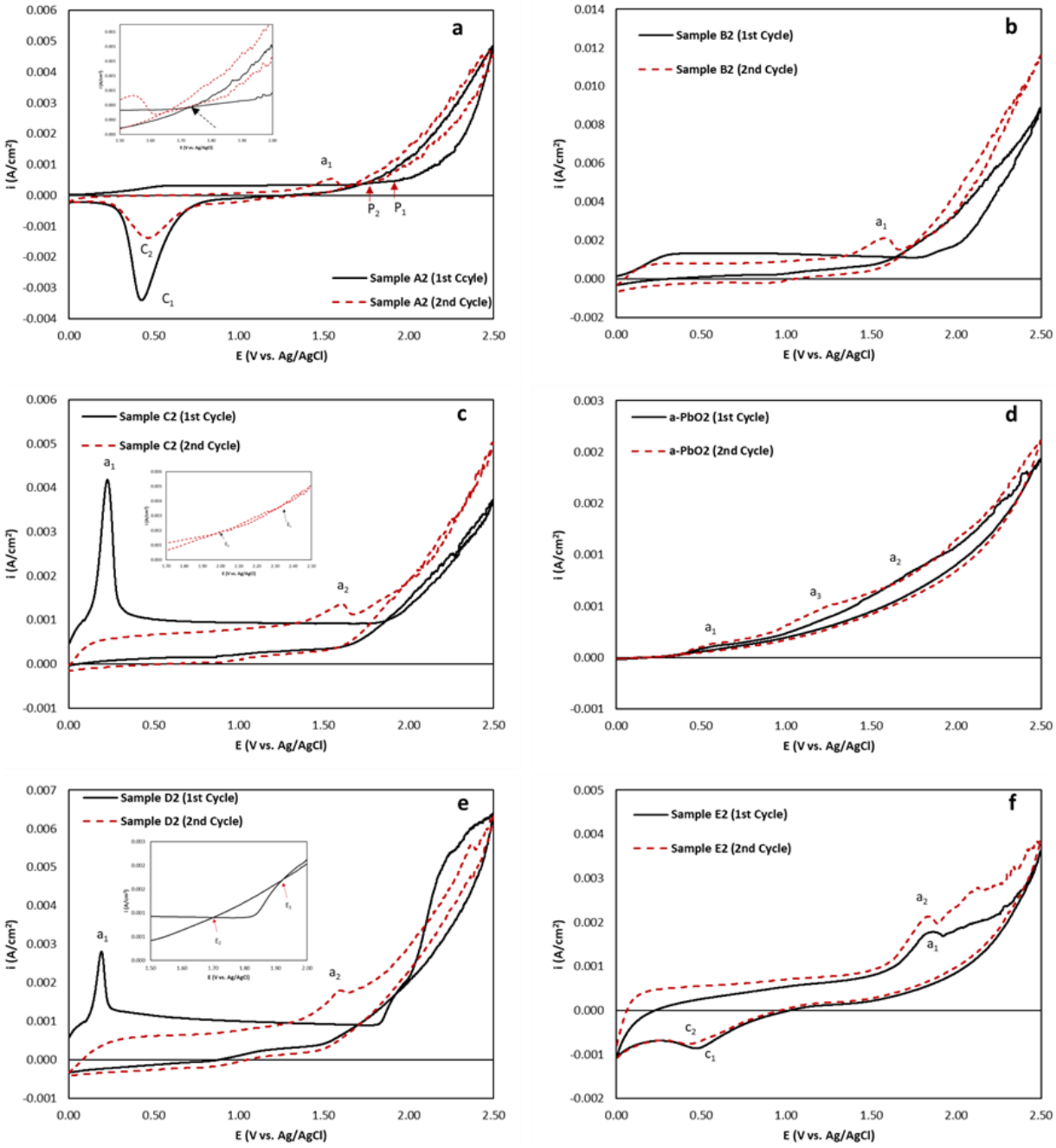

Fig. 1. Cyclic voltammetry of Ti substrate in 0.1 M HNO_3, 0.5 M $Pb(NO_3)_2$ and a) Sample A2, b) Sample B2, c) Sample C2, d) saturated PbO in 3.5 M NaOH, e) Sample D2, f) Sample E2

Fig. 1(b) shows the CV curve of the Ti substrate in 0.1 M HNO_3, 0.5 M $Pb(NO_3)_2$, and 0.05 M NaF (Sample B2). As can be seen, the E_{onset} is 1.75 V. The decrease of the E_{onset} value by 0.15 V compared to the coating without NaF shows that the deposition rate of lead dioxide has increased, which could be due to the presence of F^- ions in the electrolyte. Fluoride ions play two important roles in the lead dioxide coating: a) the formation of the PbF_2 phase, which prevents the contact of the substrate with the electrolyte and the formation of the oxide layer (TiO_2); and b) reducing the number of active sites, which decreases the oxygen evolution rate and leads to the formation of a lead dioxide layer [21]. After the addition of NaF, the process is irreversible and there are no cathodic peaks. The second cycle is similar to the first cycle, except that the E_{onset} is 0.2 V less than that of the first cycle, which is consistent with the easy continuation of the

[DOI: 10.22068/ijmse.3513]

coating on the pre-formed lead dioxide. The maximum anodic current density increases with the addition of NaF to the medium. The maximum anodic current density indicates that the presence of fluoride ions not only improves the coating process but also greatly reduces the probability of the formation of a TiO_2 oxide layer on the substrate surface [46-48].

Fig. 1(c) shows the CV curve of Ti substrate in 0.1 M HNO_3, 0.5 M $Pb(NO_3)_2$, 0.05 M NaF, and 0.026 M $Cu(NO_3)_2$ (Sample C2). A sharp anodic peak (a1) is observed in the potential range of 0.1-0.35 V, which may be related to the oxidation of copper ions and their conversion to copper oxide or hydroxide [49-52]. The main reason for using copper is to avoid lead loss at the cathode [53, 54]. From the results of CV, unexpectedly some copper is oxidized and can be deposited on the surface of the anode together with lead dioxide. This appears to have resulted in an increase in E_{onset} in the first cycle compared to the exclusive presence of fluoride ions (1.9 V). The presence of copper oxide in the common anode/electrolyte pathway appears to affect the electron transfer potential of lead dioxide, such that a higher potential is required to initiate electron transfer from lead dioxide [55, 56]. In the second cycle, the oxidation peak of copper has completely disappeared, which may be because of copper ions' tendency for reduction on the cathode. The E_{onset} in the second cycle is 0.3 V lower than the first cycle. On the return path potential in the second cycle, in contrast to previous samples, a hysteresis loop is observed in the range of 2-2.32 V, indicating the difficulty of the nucleation process in the presence of copper ions [33, 57] (such a loop was not observed in earlier samples). The presence of copper oxide interferes with the onset of the lead dioxide nucleation process, which could be due to the presence of copper oxide on the surface of the anode. The sudden decrease in the maximum density of the anodic current in the simultaneous presence of copper and fluoride ions in the environment could be due to the presence of copper oxide and the consequent decrease in conductivity.

Fig. 1(d) shows the CV curve of the Ti substrate in saturated 3.5 M sodium hydroxide with lead oxide (PbO). As can be seen, the oxidation potential is much lower in an alkaline environment than in an acidic environment. When the potential is increased, an anodic peak is observed in the potential range of 0.5-0.6 V (a1), which is probably due to the formation of Pb_3O_4 [10]. In addition, a second peak is observed in the potential range of 1.6-1.8 V (a2), possibly due to the formation of PbO_2 [10]. It appears that, unlike an acidic environment, in an alkaline environment some of the divalent lead is converted to tetravalent lead by an electrochemical reaction, forming Pb_3O_4 (or $2PbO.PbO_2$ [58]), and the remaining PbO is converted to PbO_2 at higher potentials. In the second cycle, the oxidation of PbO to PbO_2 occurs at a lower potential (a3), as expected. Subsequently, a very thin layer of PbO_2 was deposited on this sample.

To investigate the effect of SDS on the process of the lead dioxide coating (Sample D2), 0.001 M SDS was added to the coating solution in addition to NaF and $Cu(NO_3)_2$ (Fig. 1(e)). The anodic peak in the potential range of 0.1-0.35 V is related to the oxidation of copper. The height of this peak is lower than in the sample without SDS, which could be due to the presence of SDS and its occupation of the active sites as an insoluble anionic surfactant in the medium [14, 59, 60]. As the potential continues to increase, no more peaks are observed until a potential of 1.85 V, the initial potential of the lead dioxide coating. On the return path of the first cycle, a hysteresis loop is observed in the potential range of 1.7-1.96 V, indicating the difficulty of nucleation in the presence of SDS and copper ions. SDS interferes with nucleation by occupying active sites, which is the reason for observing the hysteresis loop in the first cycle. In the second cycle, the copper oxidation peak and hysteresis loop have completely disappeared, and the initial potential of the lead dioxide coating (E_{onset}) is 0.45 V lower than in the first cycle.

Fig. 1(f) shows the CV curve of the Ti substrate in 0.1 M nitric acid together with all additives and using α-PbO_2 as interlayer (Sample E2). As the potential increases, the current density increases exponentially at a potential of 1.5 V -the lowest initial potential of lead dioxide electrodeposition compared to previous samples- indicating the simultaneous effect of additives. Moreover, the oxidation peak of copper is eliminated in this curve, which is likely due to the presence of a lead dioxide interlayer (α-PbO_2). In the second cycle, the E_{onset} is lower, and the maximum current density of the anodic peak increases, indicating an

[DOI: 10.22068/ijmse.3513]

improvement in the coating process. The anodic peaks (a1) and (a2) in the potential range of 1.6-1.8 could be due to the oxidation of PbO to PbO_2, and because of the use of Ti/α-PbO_2 as the working electrode, this peak is seen from the beginning at the first cycle.

3.2. Effects of Additives on Chronoamperometry

To understand the effect of the additives on the PbO_2 electrodeposition in the initial stages, chronoamperometry was used (Fig. 2). The current transients obtained from chronoamperometry can be divided into three regions [61]: i) the current density step, representing the double layer charging; ii) an induction period, representing the time required for PbO_2 formation; and iii) the increase in current density to a maximum and the decrease to a steady state, representing the decrease of electroactive material near the electrode and the nucleation and growth of a new phase, respectively.

Table 3 shows the j_m (maximum current density during the initial stage of lead dioxide electrodeposition) and the t_m (corresponding time). Different additives have different j_m and t_m, which means that all additives change the double-layer conformation on the electrode surface. It shows that the presence of copper ions and SDS (samples C2 and D2) inhibits the electro-crystallization of lead dioxide on the Ti plate, which is in line with CV results. The t_m and j_m in sample E2 are minimum and maximum, respectively due to the ease of coating on the already formed α-PbO_2 layer compared to the titanium substrate, which shows the effect of the interlayer on the electrodeposition process at the initial stages. Fig. 2 shows that the response time (t_m) required to reach the maximum current density (j_m) is reduced in the presence of all additives and the interlayer. This means that PbO_2 is preferentially deposited on the electrode and the simultaneous presence of additives and the interlayer can reduce the formation of by-products (reactions (2) and (3)) during the nucleation induction period and increase the amount of PbO_2 deposition, resulting in greater deposition of PbO_2 on the surface of the substrate and improving the performance of the electrode.

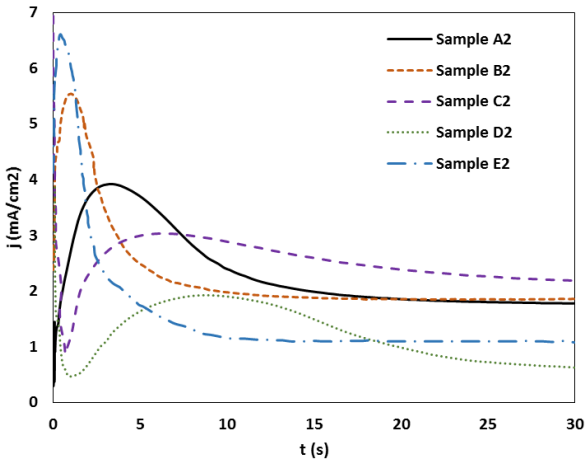

Fig. 2. Chronoamperometry curves of lead dioxide in 1.8 V (vs. Ag/AgCl) on Ti Plate (the area at 2 cm^2) in the 0.5 $mol.L^{-1}$ $Pb(NO_3)_2$ and 0.1 $mol.L^{-1}$ HNO_3 with and without different additives.

3.3. Effects of Additives on Electrochemical Impedance Spectroscopy

Fig. 3 shows the electrochemical impedance spectroscopy (EIS) of lead dioxide electrodeposition in a nitrate bath at 1.8 V vs. Ag/AgCl with different additives on the Ti plate. According to the Nyquist plot, lead dioxide with and without additives exhibits a capacitive loop at high frequencies and an inductive loop at low frequencies. The main difference between all samples is the radius of the Nyquist plot, which is larger or smaller depending on the additives used. The oxidation process in the lead nitrate bath is represented by the high-frequency capacitive loop consisting of the double-layer capacitance and the charge transfer resistance. In addition, the presence of a low-frequency inductive loop suggests the presence of an adsorbed/desorbed intermediate [62].

Table 3. t_m and j_m of Chronoamperometry curves for lead dioxide in 1.8 V (vs. Ag/AgCl) on Ti Plate (the area at 2 cm^2) in the 0.5 $mol.L^{-1}$ $Pb(NO_3)_2$ and 0.1 $mol.L^{-1}$ HNO_3 with and without different additives

Additives	t_m (s)	j_m (mA/cm^2)
Sample A2	3.22	3.92
Sample B2	1.04	5.53
Sample C2	6.67	3.03
Sample D2	8.94	1.92
Sample E2	0.40	6.60

[DOI: 10.22068/ijmse.3513]

This intermediate could be Pb(III) with oxygen, such as $Pb(OH)^{2+}$ adsorbed to the surface of the electrode [63]. Diard et al. [62] also mentioned that this loop is associated with a two-step reaction pathway that occurs at the electrode and involves the formation of an adsorbed intermediate. The reaction can be represented as follows:

Reactant → Adsorbate + e^- (Step 1)

Reactant + Adsorbate → Products + e^- (Step 2)

which can be fully associated with reactions (1) and (2).

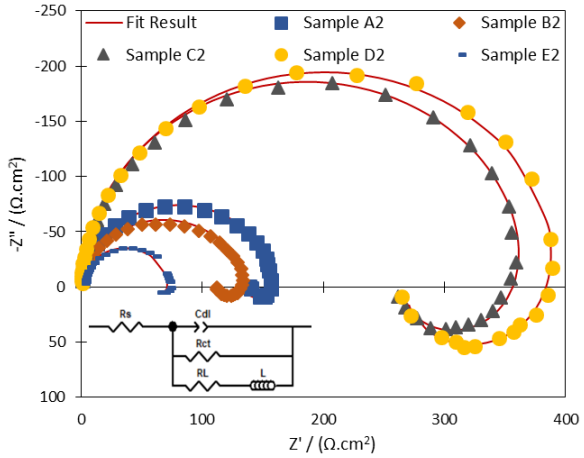

Fig. 3. Nyquist plot of lead dioxide in 1.8 V (vs. Ag/AgCl) on Ti Plate (the area at 2 cm^2) in the 0.5 $mol.L^{-1}$ $Pb(NO_3)_2$ and 0.1 $mol.L^{-1}$ HNO_3 with and without different additives.

The electrochemical equivalent circuit fitted to the Nyquist diagram, illustrated in Fig. 3. R_s describes the solution resistance, the pair Cdl/Rct represents the oxidation process, where the charge transfer resistance (Rct) is related to the reaction rate, and the capacitance of the double layer (Cdl). Part of the diagram appears in the negative imaginary part of the plot, indicating an adsorption or desorption process leading to inductive relaxation. To account for this behavior, an inductance resistance (RL) and an inductance (L) are introduced into the equivalent circuit in parallel with the Cdl/Rct pair.

According to the data calculated with the Zview2 software (Table 4), the R_{ct} values for lead dioxide in the simultaneous presence of fluoride and copper ions (Sample C2), as well as fluoride ions, copper ions, and SDS (Sample D2), are almost twice those of the lead dioxide without additives (Sample A2), showing that copper ions and SDS reduce the reaction rate. In the presence of the interlayer (Sample E2), the Rct value notably decreased, showing the essential role of the α-PbO_2 in the electrodeposition of lead dioxide. The Cdl value of lead dioxide in the presence of copper ions and SDS (Samples C2 and D2) is lower compared to lead dioxide without additives and with interlayer (Samples A2 and E2). This decrease in Cdl can be attributed to the adsorption of copper ions and SDS at the anode, which hinders the electrodeposition of lead dioxide [63].

3.4. Effects of Additives on Coating Morphology

A cyclic voltammetry method with chronoamperometry and EIS was used to investigate the mechanism and process of the reactions involved in the formation of a PbO_2 coating. SEM images of the coating surfaces are shown in Fig. 4. As can be seen in Fig. 4(a), the growth of the lead dioxide layer without additive (Sample A2) is cluster-like, indicating the superiority of vertical growth over horizontal, which is one of the reasons for the decrease in adhesion. The addition of NaF (Fig. 4(b)) leads to cohesion in the coating, and a pyramid-like structure of the lead dioxide can be seen from the beginning. The morphology of this sample is comparable to that of the samples with α-PbO_2 interlayer (Figs 4(d) and 4(f)), proving the formation of PbF_2. The presence of copper ions has led to a change in the surface structure of the coating in the first layers, significantly increasing the surface cracks and essentially transforming the coating structure into an island-like structure, similar to mixed metal oxides (MMO) anodes for oxygen evolution (Fig. 4(c)).

Table 4. Fitted EIS parameter results related to samples coated with different additives at 100 kHz – 100 mHz in 0.5 $mol.L^{-1}$ $Pb(NO_3)_2$ and 0.1 $mol.L^{-1}$ HNO_3 with 1.8 V (vs. Ag/AgCl) of applied potential.

Sample Code	Rs ($\Omega.cm^{-2}$)	Rct ($\Omega.cm^{-2}$)	n	Cdl ($\mu F.cm^{-2}$)
A2	0.35	160.60	0.95	0.118
B2	0.68	136.31	0.93	0.153
C2	0.49	371.80	1.00	0.113
D2	0.86	401.73	0.98	0.097
E2	0.90	70.33	1.00	0.242

[DOI: 10.22068/ijmse.3513]

The effects of the interlayer and SDS on the structure of the lead dioxide after the addition of α-PbO_2 interlayer and NaF can be seen in Figs 4(d) and 4(e). the presence of SDS can occupy growth sites, which significantly affects the electron/ion transfer on the surface by mechanical and electrostatic means (due to changes in the joint anode/electrolyte surface properties and consequent changes in the potential and current distribution on the anode surface), ultimately leading to a change in grain growth and the achievement of a denser surface [43]. The interlayer, on the other hand, changed the morphology of the coating from the beginning and had a significant impact on the grain size. The addition of SDS reduces the number of cracks and eliminates the island-like structure of the coating, as it is preferentially placed on active sites. The effects of all the additives in the electrolyte medium (Sample E2) on the initial layers of the lead dioxide coating can be seen in Fig. 4(f), where a very fine and dense structure influenced by the presence of NaF, the α-PbO_2 interlayer, and SDS is visible. The results show that the additives have a significant effect on the surface morphology of the coating at the initial stages.

4. CONCLUSIONS

In this study, an attempt was made to investigate the effect of three additives and one interlayer on the electrodeposition process of lead dioxide using electrochemical methods to understand their influence on lead dioxide electrodes as an oxygen evolution electrode suitable for electrowinning. The methods of cyclic voltammetry (CV), chronoamperometry (CA), and electrochemical impedance spectroscopy (EIS) were applied, and the results showed that fluoride ions not only do not interfere with the process of electrodeposition of lead dioxide but also increase the deposition rate. This could be due to the formation of PbF_2 and the prevention of oxygen evolution reaction (OER) by blocking the active sites. The presence of fluoride ions in the deposition bath also significantly reduced the probability of TiO_2 formation through the formation of a PbF_2 layer and decreased the initial potential of lead dioxide deposition. In addition, the addition of fluoride ions improved the electrodeposition of lead dioxide. It was found that copper ions, which are mainly used to prevent lead loss at the cathode, could be oxidized at the surface. On the other hand, copper ions hinder the electrodeposition of lead dioxide at the initial stages. However, the effect of copper ions is observed only in the initial stages due to their tendency to be reduced at the cathode. The presence of SDS also interfered with the deposition process by occupying the active sites. SDS as an anodic surfactant reduces the deposition rate of lead dioxide and prevents OER on the surface of the electrode. According to the present and previous studies, it can be said that SDS slightly modifies the deposition process of lead dioxide. The presence of an intermediate layer prevented copper oxidation and solved the nucleation problem. The results showed that the interlayer has the most significant effect on the electrodeposition of lead dioxide. The use of α-PbO_2 as an interlayer during electrodeposition eliminates the disadvantages of copper ions and SDS at the initial stage, and also increases the deposition rate and modifies the morphology of the electrode. Simultaneous addition of all additives and the interlayer resulted in the lowest E_{onset}, tm, and Rct values. The results indicate that the additives had a significant effect on the surface morphology in the initial deposition layers.

- Effects of F^- ions: Increases deposition rate (decrease of Rct), prevents the formation of the oxide layer (TiO_2) (The most i_{max} during CV test), changes the deposit morphology of the no-additive coating
- Effects of F^- ions + Cu^{2+} ions: Hinder lead dioxide electrodeposition and interfere with the nucleation of lead dioxide in the initial stages (copper oxidation peak and a hysteresis loop on the second cycle of CV test)
- Effects of F^- ions + Cu^{2+} ions + SDS: Hinder lead dioxide electrodeposition, interfere with the nucleation of lead dioxide (copper oxidation peak and hysteresis loop on the first cycle of CV test), decrease the deposition rate (modify the deposition process)
- Effects of F^- ions + Cu^{2+} ions + SDS on Ti/α-PbO_2: Increase the deposition rate (the lowest Rct), eliminate the effect of the presence of copper ions on the anode (elimination of copper oxidation peak and hysteresis loop), modify deposit morphology (grain size reduction on the SEM pictures)

[DOI: 10.22068/ijmse.3513]

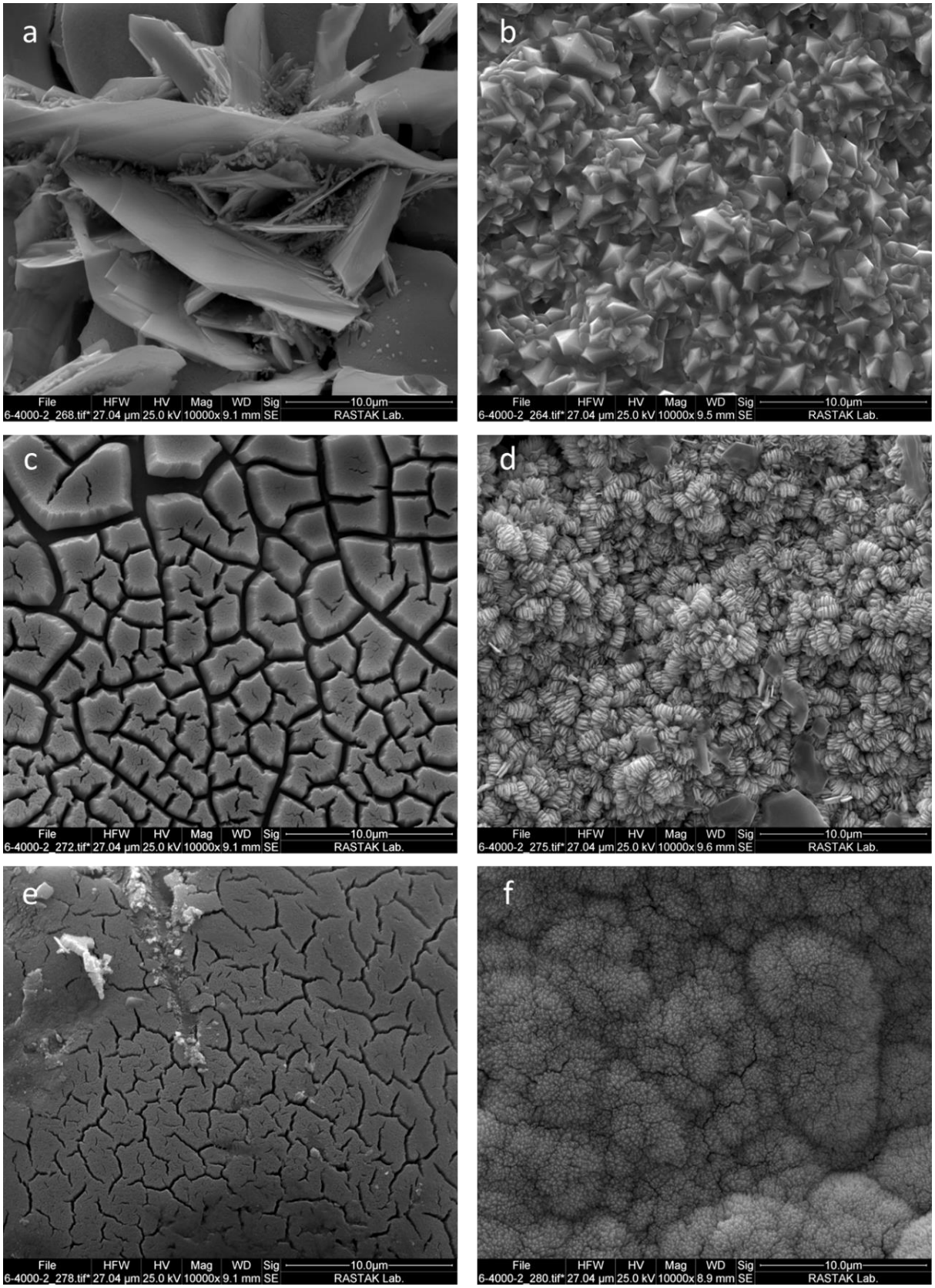

Fig. 4. SEM micrographs of samples electrodeposited in 0.1 M HNO_3, 0.5 M $Pb(NO_3)_2$ and a) Sample A2, b) Sample B2, c) Sample C2, d) Sample C2 on Ti/α-PbO_2, e) Sample D2, f) Sample E2

[DOI: 10.22068/ijmse.3513]

REFERENCES

[1] Bi, H., Yu, C., Gao, W. and Cao, P., "Physicochemical characterisation of electrosynthesized lead dioxide coatings on Ti/SnO_2-Sb substrates." Electrochimica Acta., 2013, 113, 446-453. https://doi.org/10.1016/j.electacta.2013.09.133.

[2] Boukhchina, S., Akrout, H., Berling, D. and Bousselmi, L., "Highly efficient modified lead oxide electrode using a spin coating/electrodeposition mode on titanium for electrochemical treatment of pharmaceutical pollutant." Chemosphere, 2019, 221, 356-365. https://doi.org/10.1016/j.chemosphere.2019.01.057.

[3] Wu, J., Zhu, K., Xu, H. and Yan, W., "Electrochemical oxidation of rhodamine B by PbO_2/Sb-SnO_2/TiO_2 nanotube arrays electrode." Chinese Journal of Catalysis, 2019, 40(6), 917-927. https://doi.org/10.1016/S1872-2067(19)63342-5.

[4] Dan, Y., Lu, H., Liu, X., Lin, H. and Zhao, J., "Ti/PbO^{2+} nano-Co_3O_4 composite electrode material for electrocatalysis of O2 evolution in alkaline solution." International journal of hydrogen energy, 2011, 36(3), 1949-1954. https://doi.org/10.1016/j.ijhydene.2010.11.046.

[5] Yao, Y., Zhao, C. and Zhu, J., "Preparation and characterization of PbO_2–ZrO_2 nanocomposite electrodes." Electrochimica Acta, 2012, 69, 146-151. https://doi.org/10.1016/j.electacta.2012.02.103.

[6] He, Z., Hayat, M. D., Huang, S., Wang, X. and Cao, P., "Physicochemical Characterization of PbO_2 Coatings Electrosynthesised from a Methanesulfonate Electrolytic Solution." J. Electrochem. Soc., 2018, 165(14), D1-D6. https://doi.org/10.1149/2.0161814jes.

[7] Sun, T., Wang, J., Liu, Y., Wang, J., Wang, L. and Jiang, B., "A Comprehensive Study on Nano-Diamond Doped β-PbO_2 Electrode: Preparation, Properties and Electrocatalytic Performance." Journal of The Electrochemical Society, 2019, 166(14), E473. https://doi.org/10.1149/2.0591914jes.

[8] Tang, C., Lu, Y., Wang, F., Niu, H., Yu, L. and Xue, J., "Influence of a MnO_2-WC interlayer on the stability and electrocatalytic activity of titanium-based PbO_2 anodes." Electrochimica Acta, 2020, 331, 135381. https://doi.org/10.1016/j.electacta.2019.135381.

[9] Velichenko, A., Knysh, V., Luk' Yanenko, T., Velichenko, Y. and Devilliers, D., "Electrodeposition PbO_2–TiO_2 and PbO_2–ZrO_2 and its physicochemical properties." Materials Chemistry and Physics, 2012, 131(3), 686-693. https://doi.org/10.1016/j.matchemphys.2011.10.035.

[10] Chen, B., Guo, Z., Yang, X. and Cao, Y., "Morphology of alpha-lead dioxide electrodeposited on aluminum substrate electrode." Transactions of Nonferrous Metals Society of China, 2010, 20(1), 97-103. https://doi.org/10.1016/S1003-6326(09)60103-5.

[11] Hakimi, F., Rashchi, F., Dolati, A. and Astaraei, F., "Anodizing Pb Electrode for Synthesis of β-PbO_2 Nanoparticles: Optimization of Electrochemical Parameters." Journal of The Electrochemical Society, 2019, 166(13), D617. https://doi.org/10.1149/2.0551913jes.

[12] Yao, Y., Zhou, T., Zhao, C., Jing, Q. and Wang, Y., "Influence of ZrO_2 particles on fluorine-doped lead dioxide electrodeposition process from nitrate bath." Electrochimica Acta, 2013, 99, 225-229. https://doi.org/10.1016/j.electacta.2013.03.117.

[13] Dargahi, A., Nematollahi, D., Asgari, G., Shokoohi, R., Ansari, A. and Samarghandi, M., "Electrodegradation of 2, 4-dichlorophenoxyacetic acid herbicide from aqueous solution using three-dimensional electrode reactor with G/β-PbO_2 anode: Taguchi optimization and degradation mechanism determination." RSC advances, 2018, 8(69), 39256-39268. https://doi.org/10.1039/C8RA08471H.

[14] Low, C., Pletcher, D. and Walsh, F., "The

[DOI: 10.22068/ijmse.3513]

electrodeposition of highly reflective lead dioxide coatings." Electrochemistry communications, 2009, 11(6), 1301-1304. https://doi.org/10.1016/j.elecom.2009.04.032.

[15] Yao, Y., Zhao, M., Zhao, C. and Zhang, H., "Preparation and properties of PbO_2-ZrO_2 nanocomposite electrodes by pulse electrodeposition." Electrochimica Acta, 2014, 117, 453-459. https://doi.org/10.1016/j.electacta.2013.11.150.

[16] Velichenko, A. and Devilliers, D., "Electrodeposition of fluorine-doped lead dioxide." Journal of fluorine chemistry, 2007, 128(4), 269-276. https://doi.org/10.1016/j.jfluchem.2006.11.010.

[17] Du, Y., Hao, L., Zixuan, W., Xi, W., Guirong, M. and Xu, W., "Facile synthesis of β-PbO_2 nanoparticles range from 10-30 nm and their application for ozone generation." Journal of The Electrochemical Society, 2021, 168, 123504. https://doi.org/10.1149/1945-7111/ac40c6.

[18] Du, B., Chen, Z., Yu, Q., Zhu, W., Yan, W. and Guo, Z., "Effect of temperature on the residual stress of a β-PbO_2 coating." Surface Engineering, 2018, 34(9), 689-696. https://doi.org/10.1080/02670844.2017.1391450.

[19] Liu, S., Yang, B., Zuo, A. and Tang, Y., "Characterization of a Ti/SnO_2-Sb/Fe-PVP-PbO_2 electrode deposited from methanesulfonate bath and application in electrocatalytic degradation of MO." Journal of The Electrochemical Society, 2023, 170, 092505. https://doi.org/10.1149/1945-7111/acf791.

[20] Xu, M., Gao, C., Zhang, X., Liang, X., Hu, Y. and Wang, F., "Development of SDS-modified PbO_2 anode material based on Ti^{3+} self-doping black TiO_2NTs substrate as a conductive interlayer for enhanced electrocatalytic oxidation of methylene blue." Molecules, 2023, 28(19), 6993. https://doi.org/10.3390/molecules28196993.

[21] Liu, J., Liu, F., Xu, J. and Han, Z., "Effect of current density on interface structure and performance of CF/β-PbO_2 electrodes during zinc electrowinning." Ceramics International, 2020, 46(2), 2403-2408. https://doi.org/10.1016/j.ceramint.2019.09.233.

[22] Hu, C., Liu, J., Zhang, M., Zeng, S., Guo, S., Xu, L. and Yu, L., "A novel CF/Ti/b-PbO_2 composite anode for zinc electrowinning: preparation, electrochemical properties and application." Journal of Materials Chemistry A, 2023, 11, 1403-1418. https://doi.org/10.1039/d2ta08189j.

[23] Wang, X., Wang, J., Tong, X., Wu, S., Wei, J., Chen, B., Xu, R. and Yang, L., "Constructing of Pb–Sn/α-PbO_2/β-PbO_2-Co_2MnO_4 composite electrode for enhanced oxygen evolution and zinc electrowinning." Journal of Materials Today Physics, 2023, 35, 101068. https://doi.org/10.1016/j.mtphys.2023.101068.

[24] Yin, Z., He, R., Nie, F., Wei, Z., Jia, B., Feng, Q., Fu, X. and Zhang, W., "The electrocatalysis of Mn-Co_3O_4/CeO_2@C particles with different Ce content modified Ti/PbO_2 anode and its application for copper electrodeposition." Korean Journal of Chemical Engineering, 2023, 40(12), 3059-3067. https://doi.org/10.1007/s11814-023-1538-4.

[25] Velichenko, A., Girenko, D., Kovalyov, S., Gnatenko, A., Amadelli, R. and Danilov, F., "Lead dioxide electrodeposition and its application: influence of fluoride and iron ions." Journal of Electroanalytical Chemistry, 1998, 454(1-2), 203-208. https://doi.org/10.1016/S0022-0728(98)00256-3.

[26] Velichenko, A., Amadelli, R., Zucchini, G., Girenko, D. and Danilov, F., "Electrosynthesis and physicochemical properties of Fe-doped lead dioxide electrocatalysts." Electrochimica Acta, 2000, 45(25-26), 4341-4350. https://doi.org/10.1016/S0013-4686(00)00538-7.

[27] Velichenko, A., Amadelli, R., Baranova, E., Girenko, D. and Danilov, F., "Electrodeposition of Co-doped lead dioxide and its physicochemical

[DOI: 10.22068/ijmse.3513]

properties." Journal of Electroanalytical Chemistry, 2002, 527(1-2), 56-64. https://doi.org/10.1016/S0022-0728(02)00828-8.

[28] Velichenko, A., Girenko, D. and Danilov, F., "Mechanism of lead dioxide electrodeposition." Journal of Electroanalytical Chemistry, 1996, 405(1-2), 127-132. https://doi.org/10.1016/0022-0728(95)04401-9.

[29] Velichenko, A., Amadelli, R., Benedetti, A., Girenko, D., Kovalyov, S. and Danilov, F., "Electrosynthesis and physicochemical properties of PbO_2 films." Journal of the Electrochemical Society, 2002, 149(9), C445. https://doi.org/10.1149/1.1495498.

[30] Shen, P. and Wei, X., "Morphologic study of electrochemically formed lead dioxide." Electrochimica Acta, 2003, 48(12), 1743-1747. https://doi.org/10.1016/S0013-4686(03)00149-X.

[31] Fazlinezhad, Sh., Jafarzadeh, K., Shooshtari Gugtapeh, H. and Mirali, S. M., "Characterization and electrochemical properties of stable Ni^{2+} and F^- co-doped PbO_2 coating on titanium substrate." Journal of Electroanalytical Chemistry, 2022, 909, 116145. https://doi.org/10.1016/j.jelechem.2022.116145.

[32] Kuznetsov, A. A., Kapustin, E. S., Pirogov, A. V., Kurdin, K. A., Filatova, E. A. and Kolesnikov, V. A., "An effective electrochemical destruction of non-ionic surfactants on bismuth-modified lead dioxide anodes for wastewater pretreatment." Journal of Solid State Electrochemistry, 2020, 24, 173-183. https://doi.org/10.1007/s10008-019-04483-3.

[33] Chen, S., Chen, B., Wang, S., Yan, W., He, Y., Guo, Z. and Xu, R., "Ag doping to boost the electrochemical performance and corrosion resistance of Ti/Sn–Sb-RuO_x/α-PbO_2/β-PbO_2 electrode in zinc electrowinning." Journal of Alloys and Compounds, 2020, 815, 152551. https://doi.org/10.1016/j.jallcom.2019.152551.

[34] Hao, X., Dan, S., Qian, Z., Honghui, Y. and Yan, W., "Preparation and characterization of PbO_2 electrodes from electro-deposition solutions with different copper concentration." RSC Advances, 2014, 4(48), 25011-25017. https://doi.org/10.1039/C4RA03235G.

[35] Yu, B., Xu, R., Wang, X., He, S. and Chen, B., "Electrodeposition of MnO_2-doped Pb-0.6%Sb/α-PbO_2/β-PbO_2 novel composite energy-saving anode for zinc electrowinning." Journal of Energy Storage, 2023, 61, 106264. https://doi.org/10.1016/j.est.2022.106264.

[36] Musiani, M., Fulanetto, F. and Bertoncello, R., "Electrodeposited PbO_2+RuO_2: a composite anode for oxygen evolution from sulphuric acid solution." Journal of Electroanalytical Chemistry, 1999, 465.2, 160-167. https://doi.org/10.1016/S0022-0728(99)00080-7.

[37] Jiang, W., Wang, J., Wang, X., Liao, J., Wei, J., Xu, R. and Yang, L., "Two-step facile synthesis of Co_3O_4@C reinforced PbO_2 coated electrode to promote efficient oxygen evolution reaction for zinc electrowinning." RSC Advances, 2022, 12, 10634-10645. https://doi.org/10.1039/d1ra09100j

[38] Hao, X., Quansheng, Y., Dan, S., Honghui, Y., Jidong, L., Jiangtao, F. and Wei, Y., "Fabrication and characterization of PbO_2 electrode modified with $[Fe(CN)_6]^{3-}$ and its application on electrochemical degradation of alkali lignin." Journal of Hazardous Materials, 2015, 286, 509-516. https://doi.org/10.1016/j.jhazmat.2014.12.065.

[39] Xu, P., He, X., Mao, J. and Tang, Y., "Fabrication of Ti/SnO_2-Sb/Ce-PbO_2 Anode from methanesulfonate bath and its electrocatalytic activity." Journal of The Electrochemical Society, 2019, 166(13), D638. https://doi.org/10.1149/2.1031913jes.

[40] Amadelli, R., Samiolo, L., Velichenko, A., Knysh, V., Luk'Yanenko, T. and Danilov, F., "Composite PbO_2–TiO_2 materials deposited from colloidal electrolyte: Electrosynthesis, and physicochemical properties." Electrochimica Acta, 2009, 54(22), 5239-5245. https://doi.org/10.1016/j.electacta.2009.04.024.

[41] Yao, Y., Ren, B., Yang, Y., Huang, C. and

[DOI: 10.22068/ijmse.3513]

Li, M., "Preparation and electrochemical treatment application of Ce-PbO_2/ZrO_2 composite electrode in the degradation of acridine orange by electrochemical advanced oxidation process." Journal of hazardous materials, 2019, 361, 141-151. https://doi.org/10.1016/j.jhazmat.2018.08.081.

[42] Wang, X., Xu, R., Feng, S., Yu, B. and Chen, B., "α(β)-PbO_2 doped with Co_3O_4 and CNT porous composite materials with enhanced electrocatalytic activity for zinc electrowinning." RSC advances, 2020, 10(3), 1351-1360. https://doi.org/10.1039/C9RA08032E.

[43] Sharifidarabad, H., Zakeri, A. and Adeli, M., "Parametric study on the electrochemical performance and stability of PbO_2-coated titanium electrodes for electrowinning applications." Journal of Applied Electrochemistry, 2023, 1-15. https://doi.org/10.1007/s10800-023-01867-2.

[44] Peng, H. Y., Chen, H. Y., Li, W. S., Hu, S. J., Li, H., Nan, J. M. and Xu, Z. H., "A study on the reversibility of Pb (II)/PbO_2 conversion for the application of flow liquid battery." Journal of power sources, 2007, 168(1), 105-109. https://doi.org/10.1016/j.jpowsour.2006.11.016.

[45] Darabizad, G., Rahmanifar, M. S., Mousavi, M. F. and Pendashteh, A., "Electrodeposition of morphology-and size-tuned PbO_2 nanostructures in the presence of PVP and their electrochemical studies." Materials Chemistry and Physics, 2015, 156, 121-128. https://doi.org/10.1016/j.matchemphys.2015.02.037.

[46] Duan, X., Ma, F., Yuan, Z., Chang, L. and Jin, X., "Electrochemical degradation of phenol in aqueous solution using PbO_2 anode." Journal of the Taiwan Institute of Chemical Engineers, 2013, 44(1), 95-102. https://doi.org/10.1016/j.jtice.2012.08.009

[47] Mohd, Y. and Pletcher, D., "The fabrication of lead dioxide layers on a titanium substrate." Electrochimica acta, 2006, 52(3), 786-793. https://doi.org/10.1016/j.electacta.2006.06.013.

[48] An, H., Li, Q., Tao, D., Cui, H., Xu, X., Ding, L., Sun, L. and Zhai, J., "The synthesis and characterization of Ti/SnO_2–Sb_2O_3/PbO_2 electrodes: the influence of morphology caused by different electrochemical deposition time." Applied Surface Science, 2011, 258(1), 218-224. https://doi.org/10.1016/j.apsusc.2011.08.034.

[49] Drissi-Daoudi, R., Irhzo, A. and Darchen, A., "Electrochemical investigations of copper behaviour in different cupric complex solutions: Voltammetric study." Journal of Applied Electrochemistry, 2003, 33(3), 339-343. https://doi.org/10.1023/A:1024191404595

[50] Cong, H., Michels, H. and Scully, J. R., "Passivity and pit stability behavior of copper as a function of selected water chemistry variables." ECS Transactions, 2009, 16(52), 141. https://doi.org/10.1149/1.3229963.

[51] Zhang, Z. and Wang, P., "Highly stable copper oxide composite as an effective photocathode for water splitting via a facile electrochemical synthesis strategy." Journal of Materials Chemistry, 2012, 22(6), 2456-2464. https://doi.org/10.1039/C1JM14478B,

[52] Giri, S. D. and Sarkar, A., "Electrochemical study of bulk and monolayer copper in alkaline solution." Journal of The Electrochemical Society, 2016, 163(30), H252. https://doi.org/10.1149/2.0071605jes.

[53] Li, X., Pletcher, D. and Walsh, F. C., "Electrodeposited lead dioxide coatings." Chemical Society Reviews, 2011, 40(7), 3879-3894. https://doi.org/10.1039/C0CS00213E.

[54] Narasimham, K. and Udupa, H., "Preparation and applications of graphite substrate lead dioxide (GSLD) anode." Journal of the Electrochemical Society, 1976, 123(9), 1294. https://doi.org/10.1149/1.2133063.

[55] Bozzini, B., Mele, C., D'urzo, L. and Romanello, V., "An electrochemical and in situ SERS study of Cu electrodeposition from acidic sulphate solutions in the presence of 3-diethylamino-7-(4-dimethylaminophenylazo)-5-phenylphenazinium chloride (Janus Green

[DOI: 10.22068/ijmse.3513]

B).” Journal of applied electrochemistry, 2006, 36(9), 973-981. https://doi.org/10.1007/s10800-006-9124-0.

[56] Hubin, A., Gonnissen, D., Simons, W. and Vereecken, J., “Spectro-electrochemical study of the influence of ligand adsorption on the reaction rate of the electrodeposition of silver complexes.” Journal of Electroanalytical Chemistry, 2007, 600(1), 142-150. https://doi.org/10.1016/j.jelechem.2006.05.017

[57] Zhang, J., An, M., Chen, Q., Liu, A., Jiang, X., Ji, S., Lian, Y. and Wen, X., “Electrochemical study of the diffusion and nucleation of gallium (III) in [Bmim] [TfO] ionic liquid.” Electrochimica Acta, 2016, 190, 1066-1077. https://doi.org/10.1016/j.electacta.2016.01.027

[58] Dickens, B., “The bonding in Pb_3O_4 and structural principles in stoichiometric lead oxides.” Journal of Inorganic and Nuclear Chemistry, 1965, 27(7), 1509-1515. https://doi.org/10.1016/0022-1902(65)80011-2.

[59] Kozarac, Z., Nikolić, S., Ružić, I. and Ćosović, B., “Inhibition of the electrode reaction in the presence of surfactants studied by differential pulse polarography: Cadmium (II) in seawater in the presence of the Triton-X-100.” Journal of Electroanalytical Chemistry and Interfacial Electrochemistry, 1982, 137(2), 279-292. https://doi.org/10.1016/0022-0728(82)80043-0.

[60] Felhősi, I., Telegdi, J., Pálinkás, G., and Kálmán, E., “Kinetics of self-assembled layer formation on iron.” Electrochimica Acta, 2002, 47(13-14), 2335-2340. https://doi.org/10.1016/S0013-4686(02)00084-1.

[61] Knysh, V., Luk’yanenko, T., Shmychkova, O., Amadelli, R. and Velichenko, A., “Electrodeposition of composite PbO_2–TiO_2 materials from colloidal methanesulfonate electrolytes.” Journal of Solid State Electrochemistry, 2017, 21, 537-544. https://doi.org/10.1007/s10008-016-3394-1.

[62] Diard, J. P., Le Gorrec, B. and Montella, C., “Calculation, Simulation and interpretation of electrochemical impedances: Part 3. Conditions for observation of low frequency inductive diagrams for a two-step electron transfer reaction with an adsorbed intermediate species.” Journal of Electroanalytical Chemistry, 1992, 326(1-2), 13-36. https://doi.org/10.1016/0022-0728(92)80500-4.

[63] Yao, Y., Cui, L., Zhao, C. and Jiao, L., “Influences of cerium on the electrodeposition process and physicochemical properties of lead dioxide electrodes.” Journal of The Electrochemical Society, 2014, 161(10), D528-D533. https://doi.org/10.1149/2.0901410jes.

[DOI: 10.22068/ijmse.3513]